CHEMISTRY OF MATERIALS
Article

Chem. Mater. **2010,** *22,* 1297–1308 1297
DOI:10.1021/cm9034402

Observation of Hybrid Carbon Nanostructures as Intermediates in the Transformation from Hydrocarbon Nanotubes and Nano-onions to Carbon Nanotubes and Nano-onions via Sonolysis on Silicon Nanowires and Nanodots, Respectively

Boon K. Teo,*[,†] X. H. Sun,*[,‡] C. P. Li,[§,⊥] N. B. Wong,[§,||] and S. T. Lee[§,⊥]

[†]*Department of Chemistry, University of Illinois at Chicago, 845 West Taylor Street, Chicago, Illinois 60607,* [‡]*Functional Nano & Soft Materials (FUNSOM) Laboratory, Soochow University, Suzhou, P.R. China,* [§]*Center of Super-Diamond & Advanced Film (COSDAF),* [⊥]*Department of Physics and Materials Science, and* [||]*Department of Biology and Chemistry, City University of Hong Kong, Hong Kong SAR, China*

Received April 14, 2009. Revised Manuscript Received December 4, 2009

It was found that hydrocarbon nanotubes (HCNTs) and nano-onions (HCNOs) (hereafter collectively referred to as HCNT(O)s) can be converted to carbon nanotubes (CNTs) and nano-onions (CNOs) (hereafter collectively referred to as CNT(O)s) upon prolonged sonication via hybrid CNT⊂HCNT and CNO⊂HCNO nanostructures as intermediates, respectively. These intermediate hybrid carbon nanostructures may thus be considered as snapshots in the transformation process. The morphologies and the characteristic properties of these carbon nanostructures are reported. The formation of HCNT(O)s, and their subsequent transformation from HCNT(O)s to the hybrid CNT(O)⊂HCNT(O) nanostructures, and ultimately to the conventional CNT(O)s, have been elucidated by recording the HRTEM images of the products as a function of sonication time and in different solvents. On the basis of these experimental results, detailed formation mechanism and transformation pathways of these carbon nanomaterials, as well as their interrelationships, are proposed. Structural models of the HCNTs and HCNOs are also proposed. Other peculiar phenomena and transformation processes of these nanomaterials are also described.

Introduction

We recently reported a simple, one-step sonochemical synthetic method to produce carbon nanomaterials from common organic solvents using hydrogen-passivated silicon nanowires (SiNWs) and nanodots (SiNDs) as templates ("nanomolds") under ambient conditions (room temperature and atmosphere pressure).[1,2] In addition to the conventional carbon nanotubes (CNTs) and nano-onions (CNOs), with uniform interlayer spacing of 3.4 Å, a new class of carbon nanomaterials, which were described as hydrocarbon nanotubes (HCNTs) and nano-onions (HCNOs), was also observed. These latter carbon nanomaterials exhibit variable interlayer spacing ranging from ca. 4 to 6 Å. Because many common organic solvents can be used, this synthetic route opens the door to facile synthesis of various carbon nanostructures. This technique has the advantage that it requires neither specialized equipment nor metal catalysts for the preparation.

This paper reports a hitherto unreported form of carbon nanostructures which may be described as the hybrid of conventional carbon nanotubes (CNTs) and hydrocarbon nanotubes (HCNTs) as well as that of conventional carbon nano-onions (CNOs) and hydrocarbon nano-onions (HCNOs). More importantly, in our sonosynthesis of HCNTs and HCNOs on SiNWs and SiNDs (hereafter referred to collectively as SiNW(D)s), respectively, via ultrasonication, we discovered that HCNTs and HCNOs (hereafter referred to collectively as HCNT(O)s) can be converted to CNTs and CNOs (hereafter referred to collectively as CNT(O)s), respectively, upon prolonged sonication. It can therefore be inferred that these hybrid carbon nanostructures are intermediates in the transformation process. In this paper, we describe the morphologies and properties of these new hybrid nanostructures and their relationships to the formation and transformation pathways of these carbon nanomaterials. To shed light on the genesis of the formation of HCNT(O)s, and the subsequent transformation from HCNT(O)s to the hybrid CNT(O)⊂HCNT(O) nanostructures, and ultimately to the conventional CNT(O)s, the HRTEM images of the products were recorded as a function of sonication time and in different solvents. On the basis of the structural evolution of the products, detailed formation mechanism and transformation pathways of these carbon nanomaterials, as well as their interrelationships, are proposed in this paper. Structural models of the HCNT(O)s are also discussed. Other

*To whom correspondence should be addressed. E-mail: boonkteo@uic.edu (B.K.T.); xhsun@suda.edu.cn (X.H.S.).

(1) Sun, X. H.; Li, C. P.; Wong, N. B.; Lee, C. S.; Lee, S. T.; Teo, B. K. *J. Am. Chem. Soc.* **2002**, *124*, 14856.
(2) Li, C. P.; Teo, B. K.; Sun, X. H.; Wong, N. B.; Lee, S. T *Chem. Mater.* **2005**, *17*, 5780.

Published on Web 01/11/2010

peculiar phenomena and transformation processes of these carbon nanomaterials are also discussed.

Experimental Section

SiNWs were synthesized by thermal evaporation of SiO powders as described in the literature.[3] SiNWs were oxide-removed and H-passivated by etching with an aqueous (5%) HF solution for five minutes.[4] Typically, the HCNTs and HCNOs were produced by dispersing ca. 1 mg of HF-etched SiNW(D)s in 5−10 mL of selected common organic solvents such as $CHCl_3$, CH_2Cl_2, CH_3I, etc. (categorized as Class A solvents to be defined below), followed by bath sonication for 15 min in a common laboratory ultrasonic cleaner (40 kHz) under ambient conditions (room temperature and pressure). The golden yellowish solution turned turbid within minutes of sonication and exhibited the Tyndal effect characteristic of colloidal solutions. A few drops of the resulting solution were put onto a lacey carbon film and characterized by high-resolution transmission electron microscopy (HRTEM, Philips CM200 FEG, operated at 200 KeV). The results are shown in Figures 1−3 (with $CHCl_3$ as solvent). All containers or spatulas used were made of Teflon and all solvents used were reagent grade. Triply distilled water was used in preparing the HF solution.

To probe the genesis of the formation of HCNTs, and the subsequent transformation from HCNTs to the hybrid CNT⊂HCNT nanostructures, and ultimately to the conventional CNTs, we studied the HRTEM images of HF-etched (as described above) SiNWs in $CHCl_3$ as a function of sonication time, namely, from 0 to 20 min at 5 min intervals. This was done by withdrawing a few drops of the solution (prepared via the sample preparation procedure described above for Figures 1−3) after a specific time interval. The results are depicted in Figure 4a−e. Figure 4a was obtained via mechanical stirring (with the aid of a magnetic stirrer) only. A similar study was performed on HF-etched (via the sample preparation procedure described above for Figures 1−3) SiNWs in benzene as a function of sonication time, namely, from 10 to 20 to 30 min. The results are shown in Figure 5a−c, respectively.

The sample for Raman study was prepared as follows. Approximately 1 mg of SiNWs (after treatment with a 5% HF aqueous solution[4]) was dispersed in 2 mL of $CHCl_3$. The solution was sonicated for 15 min in a common laboratory ultrasonic cleaner (40 kHz) under ambient conditions. A few drops of the resulting solution were dropped onto a glass slide and dried in the air. This procedure was repeated many times until approximately 1 mL of solution was evaporated to produce a thin solid film of 1 cm in diameter. Within the film, small bundles of SiNWs were observed. The sample was subsequently examined by Raman spectroscopy using a Renishaw micro-Raman spectrometer at room temperature. Excitation was by means of the 514 nm line of an Ar^+ laser, and the Raman signals were measured in a backscattering geometry with a spectral resolution of 1.0 cm^{-1}. The resulting spectrum is shown in Figure 6.

For FTIR measurements, 1 mg of HF-treated[4] SiNWs was dispersed in 2 mL of $CHCl_3$ and sonicated for 30 min. The turbid golden solution was dispersed onto a GaAs wafer and dried in a nitrogen stream. This procedure was repeated several times until approximately 1 mL solution was evaporated to produce a thin solid film of 1 cm in diameter. Within the film, small bundles of SiNWs were observed. The sample was stored under nitrogen until FTIR measurements (in the microattenuated total reflection (ATR) mode). The ATR-FTIR measurements was performed in air using a Perkin-Elmer Spectrum One FTIR spectrometer interfaced to an i-Series FTIR microscope equipped with a HgCdTe detector cooled with liquid nitrogen. The micro-ATR objective is a germanium crystal with a probe size of 100 μm in diameter. The resolution of the spectra was 2 cm^{-1}. The resulting spectrum is shown in Figure 7.

Finally, Figure 8 was obtained with chloroform as solvent and Figure 9a−c was from methylene chloride, both via the sample preparation procedure described above for Figures 1−3.

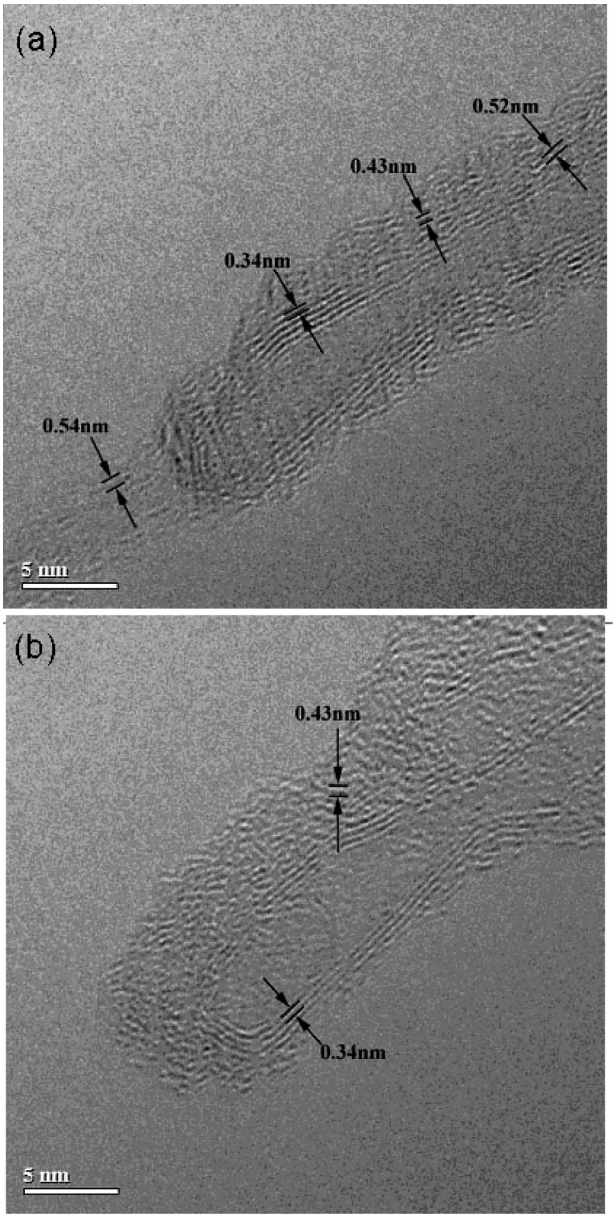

Figure 1. Two high-resolution TEM (HRTEM) images of hybrid carbon nanotubes, the inner layers are conventional CNT with interlayer spacing of 3.4 Å and the outer layers are hydrocarbon layers with interlayer spacing ranging from 4 to 6 Å, both with $CHCl_3$ as solvent.

Results and Discussion

It was during an attempt to disperse HF-etched SiNWs in common organic solvents under sonication at ambient conditions that we discovered a variety of new,

(3) Lee, S. T.; Wang, N.; Zhang, Y. F.; Tang, Y. H. *MRS Bull.* **1999**, *24*, 36.
(4) Sun, X. H.; Wang, S. D.; Wong, N. B.; Ma, D. D. D.; Lee, S. T.; Teo, B. K. *Inorg. Chem.* **2003**, *42*, 2398.

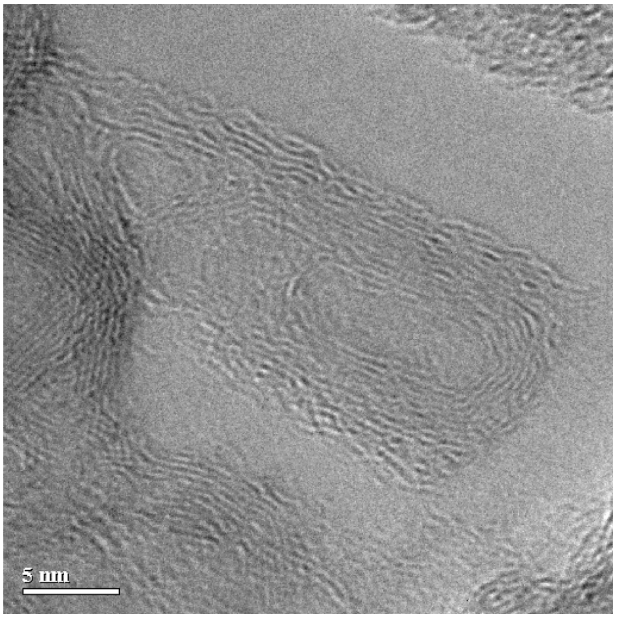

Figure 2. A HRTEM image of a hybrid bamboo-like HCNT/CNT from $CHCl_3$. Note that the inner layers are like CNTs (with interlayer spacing of 3.4 Å), whereas the outer layers resemble HCNTs (with interlayer spacing ranging from 4 to 6 Å).

structurally well-defined, hydrocarbon nanomaterials. They include: hydrocarbon nanotubes (HCNTs) and hydrocarbon nano-onions (HCNOs), and the conventional carbon nanotubes (CNT) and carbon nano-onions (CNOs). These carbon nanomaterials are products of sonochemical reactions between HF-etched SiNWs and SiNDs and the organic solvent molecules, respectively. The important feature is that these carbon nanomaterials can be prepared under ambient conditions (room temperature and atmospheric pressure). We note that conventional carbon nanotubes (CNTs) and nano-onions (CNOs) are commonly produced by such diverse techniques as arc discharge,[5] laser ablation,[6] chemical vapor deposition (CVD),[7] electron beam irradiation and high temperature annealing,[8,9] etc., most of which require severe conditions such as high temperature, high vacuum, high voltage arc discharge, or high-energy electron irradiation. Many of these techniques also require sophisticated equipment such as lasers and chemical vapor deposition (CVD). Some also require metal catalysts for growth which may be an issue in the subsequent use of these nanomaterials. Room-temperature synthesis of CNTs and CNOs is rare, though there were reports of the fabrication of CNTs[10] and CNOs[11] by arc discharge (using graphite electrodes) in water at room temperature. Syntheses of CNTs and

(5) Iijima, S. *Nature* **1991**, *354*, 56.
(6) Thess, A.; Lee, R.; Nikolaev, P.; Dai, H. J.; Petit, P.; Robert, J.; Xu, C. H.; Lee, Y. H.; Kim, S. G.; Rinzler, A. G.; Colbert, D. T.; Scuseria, G. E.; Tomanek, D.; Fischer, J. E.; Smalley, R. E. *Science* **1996**, *273*, 483.
(7) Kong, J.; Cassell, A. M.; Dai, H. J. *Chem. Phys. Lett.* **1998**, *292*, 567.
(8) De Heer, W. A.; Ugarte, D. *Chem. Phys. Lett.* **1993**, *207*, 480.
(9) Ugarte, D. *Nature* **1992**, *359*, 707.
(10) Hsin, Y. L.; Hwang, K. C.; Chen, F. R.; Kai, J. J. *Adv. Mater.* **2001**, *13*, 830.
(11) Sano, N.; Wang, H.; Chhowalla, M.; Alexandrou, I.; Amaratunga, G. A. J. *Nature* **2001**, *414*, 505.

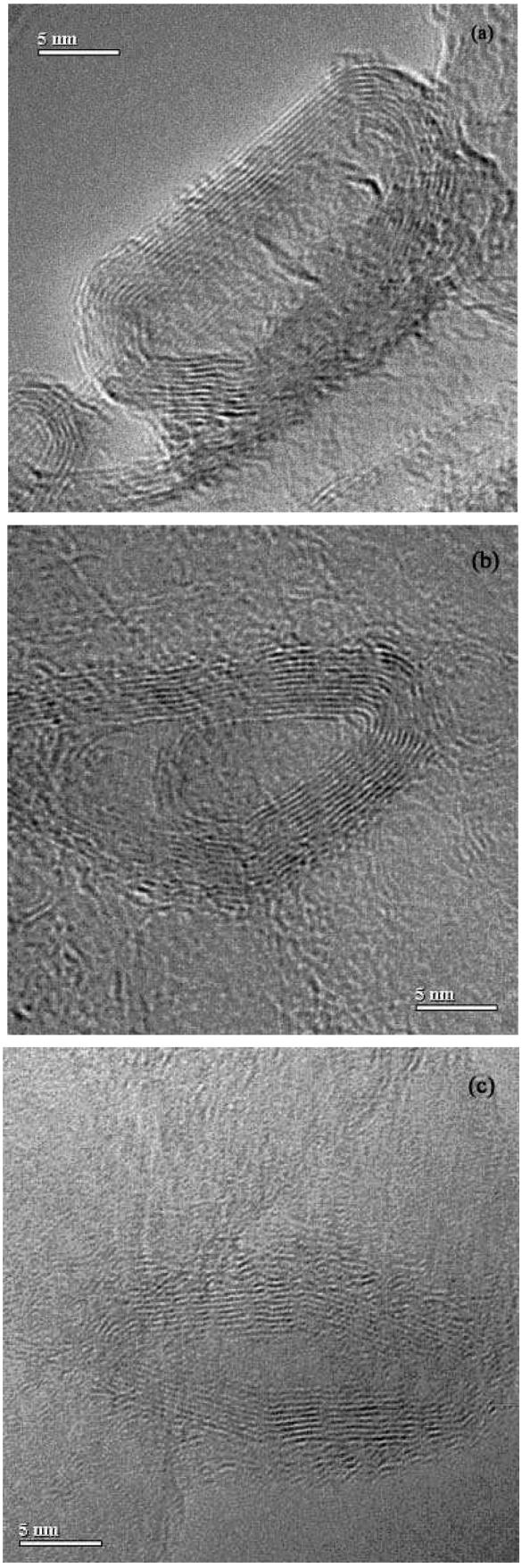

Figure 3. HRTEM images of hybrid HCNOs of different topologies (with $CHCl_3$ as solvent): (a) a sealed capsule (rounded rectangle), (b) a rounded triangle (bamboo-like), and (c) a diamond-shaped nanostructure.

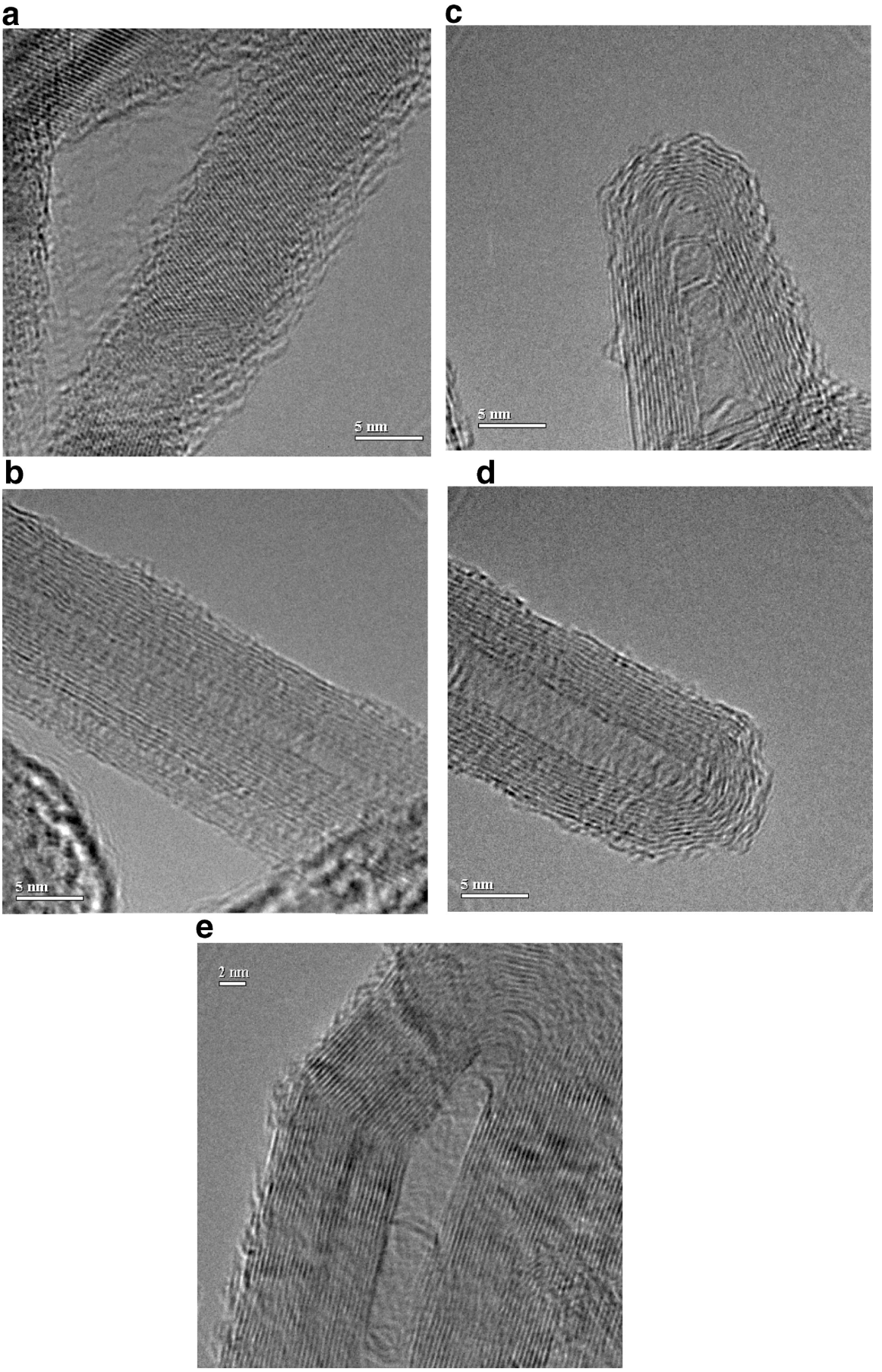

Figure 4. HRTEM images of HF-etched SiNWs in $CHCl_3$ as a function of sonication time, namely: (a) 0 (mechanical stirring only), (b) 5, (c) 10, (d) 15, and (e) 20 min.

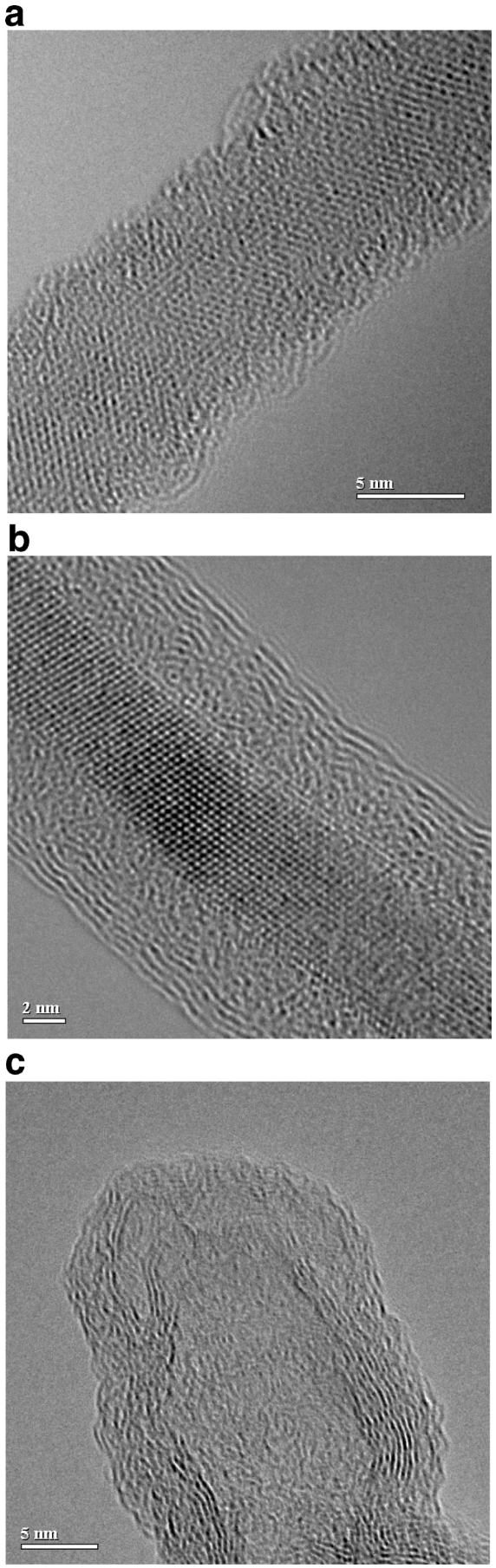

Figure 5. HRTEM images of HF-etched SiNWs in benzene as a function of sonication time, namely: (a) 10, (b) 20, and (c) 30 min.

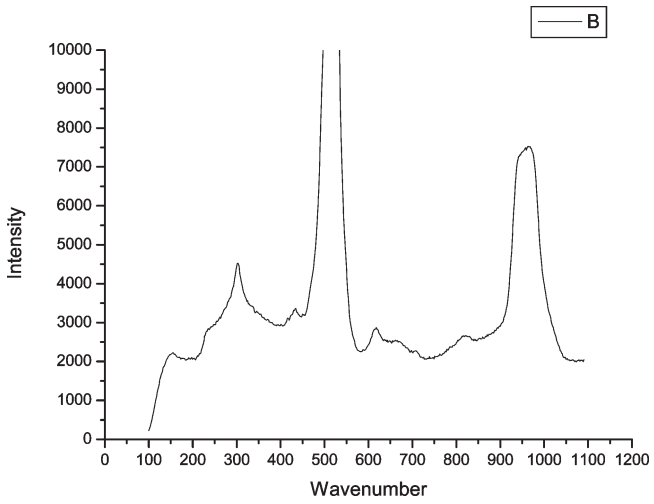

Figure 6. Raman scattering spectra, in the 100−1100 cm^{-1} region, of HCNT/CNT on SiNWs synthesized from a $CHCl_3$ solution.

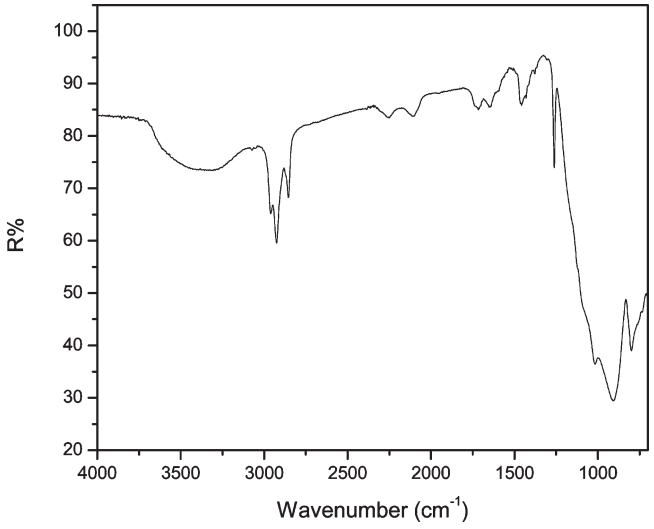

Figure 7. FTIR of as-prepared HCNT/CNT on SiNWs (SiNWs was etched with 5% HF for 20 min and sonicated in $CHCl_3$ for 30 min).

CNOs via sonolysis are also rare, though, subsequent to our first Communication[1] in 2002, there was a report in 2004 of a similar sonication method for the synthesis of single-walled carbon nanotubes on the surface of the silica powder in *p*-xylene.[12] This method, however, requires ferrocene as the precursor of the Fe catalyst and silica powder as the nucleation site.

Structurally well-defined HCNTs and HCNOs are rare commodities. To the best of our knowledge, our sonochemical method is the first report of the facile synthesis of multiwalled HCNTs and HCNOs under ambient conditions.[1] Partial hydrogenation of single-walled CNTs, giving rise to deformed or cut (etched) hydrocarbon nanotubes, were reported in the literature using highly reactive atomic hydrogen generated from rf frequency[13,14]

(12) Jeong, S.-H.; Ko, J.-H.; Park, J.-B.; Park, W. *J. Am. Chem. Soc.* **2004**, *126*, 15982.
(13) Nikitin, A; Ogasawara, H.; Mann, D.; Denecke, R.; Zhang, Z.; Dai, H.; Cho, K.; Nilsson, A. *Phys. Rev. Lett.* **2005**, *95*, 225507.
(14) Zhang, G.; Qi, P.; Wang, X.; Lu, Y.; Mann, D.; Li, X.; Dai, H. *J. Am. Chem. Soc.* **2006**, *128*, 6026.

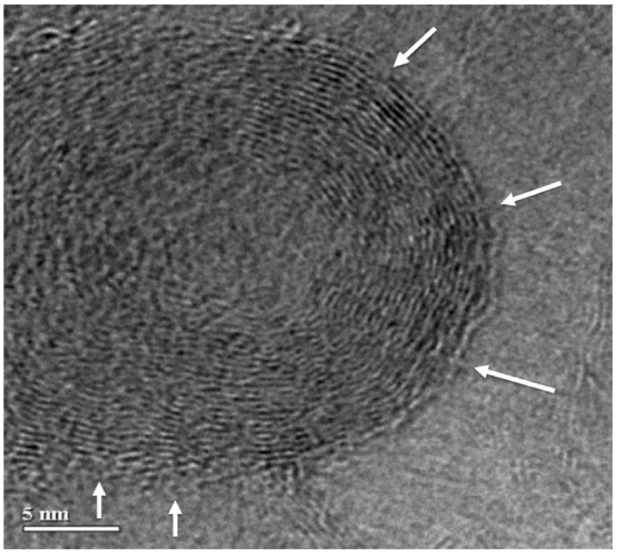

Figure 8. HRTEM image of a hybrid HCNO/CNOs (with $CHCl_3$ as solvent) showing the ultrasonic explosion. Note that three or four outer layers of the nano-onion are wavy, indicative of the HCNO structure, whereas the inner layers are smooth, suggesting a CNO interior.

or glow discharge[15] (hydrogen plasma). The reverse dehydrogenation reaction also requires harsh conditions such as high-temperature treatment at 500−600 °C.[13−15]

We believe that the simple one-step sonofabrication route reported by us[1,2,16] opens the door to facile synthesis of hydrogenated carbon nanotubes and nano-onions, along with the conventional carbon nanotubes and nano-onions under mild conditions (at room temperature and atmospheric pressure).

These carbon nanomaterials exhibit a wide variety of shapes and forms, with the most common ones being the multiwalled nanotubes and nano-onions. A gallery of representative morphologies of multiwalled HCNTs and CNTs as well as multiwalled HCNOs and CNOs can be found in ref 2. (Throughout this paper, it is understood that all the carbon nanostructures produced by the present method are "multi-walled."). It can be seen from Figure 2 of ref 2 that conventional CNTs thus produced have uniform interlayer spacing of 3.4 Å, whereas the corresponding HCNTs have variable interlayer spacing of 4−6 Å. The number of layers generally ranges from 3 to 20. Both of these products were formed upon sonication of SiNWs dispersed in selected common organic solvents such as chloroform or methylene chloride under ambient conditions. Similarly, HCNOs and CNOs can likewise be formed with SiNDs as templates.

In this paper, we report a hitherto unreported new class of hybrid HCNT(O)/CNT(O) nanostructures, along with their morphological differences and spectroscopic properties. These hybrid nanostructures can be considered as intermediates between HCNT(O)s and CNT(O)s. In fact, as we shall see later, upon prolonged sonication, HCNT(O)s can be converted into CNT(O)s, suggesting that

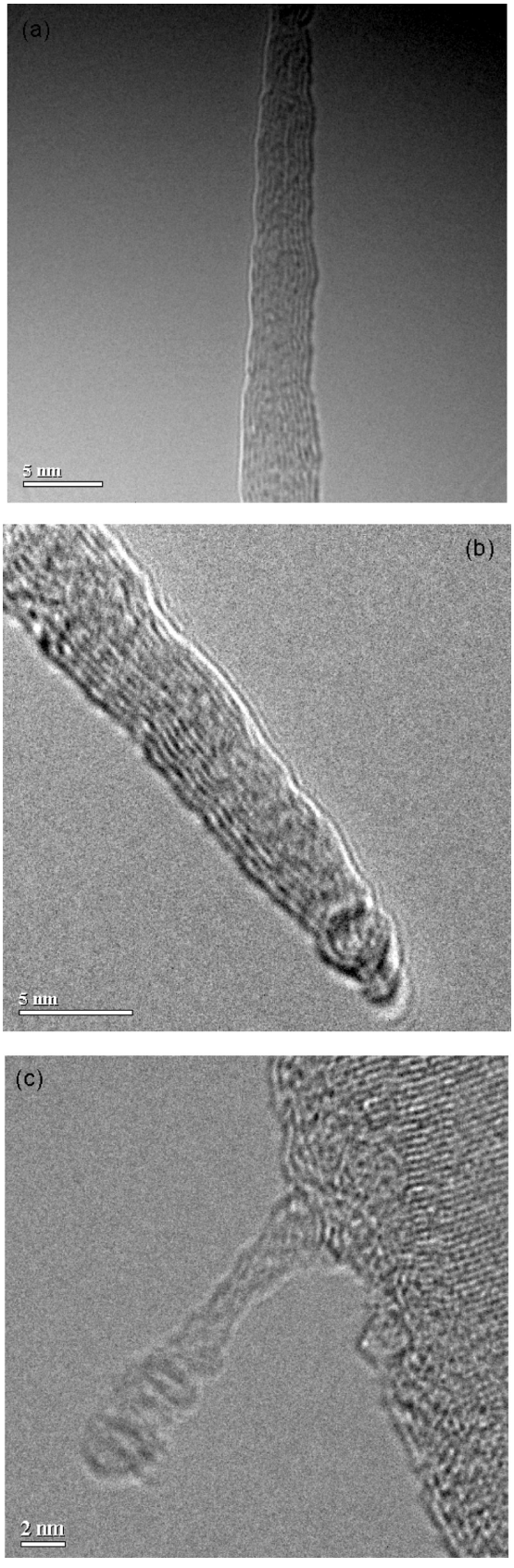

Figure 9. HRTEM images of a "self-healing" process of HCNT (from CH_2Cl_2) under intense electron beam irradiation during the TEM observation: (a) an original HCNT before electron beam irradiation; (b) one example of the self-sealed fused "caps" at the cleaved ends of the HCNT after cutting by electron beam irradiation, (c) a separate, badly damaged, sealed-off HCNT tube hanging off a SiNW after cleaving by prolonged electron beam irradiation.

(15) Khare, B. N.; Meyyappan, M.; Cassell, A. M.; Nguyen, C. V.; Han, J. *Nano Lett* **2002**, *2*, 73–77.
(16) Lee, S. T.; Li, C. P.; Sun, X. H.; Wong, N. B.; Lee, C. S.; Teo, B. K. U.S. Patent **2006**, no. 7 132 126.

these hybrid nanostructures are intermediates in the transformation process.

A. Morphologies of Hybrid Carbon Nanostructures. (*1*) *Hybrid HCNT/CNTs*. Images a and b in Figure 1 depict the HRTEM pictures of two hybrid HCNT/CNTs. These hybrid nanostructures are intermediates in the transformation from HCNTs to CNTs and thus represent snapshots of the transformation in progress. It can be seen that the smooth CNT layers with an interlayer spacing of 3.4 Å are covered by wavy hydrocarbon layers, with interlayer spacing ranging from 4.3 to 5.4 Å. The observation of these hybrid HCNT/CNTs is significant in that it may shed light on the mechanism of formation of these nanostructures (vide infra). Similarly, hybrid HCNO/CNOs of various morphologies were observed as we shall see in the following subsections.

(*2*) *Bamboo-like HCNT/CNTs*. In addition to hybrid carbon nanotubes and nano-onions, some peculiar morphologies of hybrid carbon nanostructures were also observed. For example, a bamboo-like hybrid HCNT/CNT is depicted in Figure 2, which can be described as a sealed cone-shaped tube with compartmentalized hollow cavities.

(*3*) *Hybrid HCNO/CNOs*. Various kinds of hybrid carbon nano-onion or nanoshell structures can also be found. A few representative shapes are shown in Figure 3a−c. The nanostructure in Figure 3a may be visualized as a truncated rectangle (or a short multiwalled nanotube sealed on both ends). The nanostructures in images b and c in Figure 3 may be described as rounded triangular and diamond shapes, respectively.

B. Characteristics of HCNT(O)s and Hybrid HCNT(O)/CNT(O) Nanostructures. As described previously,[2] the characteristics of HCNT(O)s, which distinguish them from the conventional CNT(O)s, are: (1) wavy layers or shells; (2) large and variable interlayer spacing ranging from ca. 4 to 6 Å; (3) prolonged sonication can convert HCNT(O) into CNT(O)s; (4) partially hydrogenated; the degree of hydrogenation decreases with the sonication time; and (5) HCNT(O)s are easily shrunk, buckled, damaged, or broken by intense electron beam. These characteristics are also found in the HCNT(O) parts (outer layers) of the hybrid HCNT(O)/CNT(O) nanostructures.

C. Four Key Components of the Synthesis of HCNT(O)s, CNT(O)s, and the Hybrids. There are four key components in the sonochemical synthesis of HCNT(O)s, CNT(O)s, and the hybrid intermediates. Lacking any of these components or factors will lead to no production or very low yield of the products. We shall describe each of these factors with appropriate experimental evidence.

(*1*) *The Energy Source: Sonication*. It is believed that sonication provides the energy needed for the formation of these HCNTs/HCNOs. In fact, sonication not only promotes the heterogeneous reaction between the SiH_x moieties on the SiNW surfaces and the organic molecules in solution, but also causes the extrusion (or demolding) of the products from the SiNWs/SiNDs, respectively. Such transformations and/or processes are made possible owing to the fact that acoustic cavitation of ultrasound can induce local heating to temperatures as high as 5200 K with lifetimes of $< 1\ \mu s$.[17]

To shed light on the genesis of the formation of HCNTs and the subsequent transformation from HCNTs to the hybrid CNT⊂HCNT nanostructures and ultimately to the conventional CNTs, we studied the HRTEM images of HF-etched SiNWs in $CHCl_3$ as a function of sonication time, namely, from 0 to 20 min at 5 min intervals. The results are depicted in Figure 4a−e. In particular, Figure 4a was obtained via mechanical stirring (with the aid of a magnetic stirrer) only. It can be seen that only an amorphous carbon layer was obtained. HCNTs (Figure 4b) were formed after 5 min sonication. Further sonication progressively transformed HCNTs to the hybrid CNT⊂HCNT nanostructures (Figure 4d,e) and eventually to the conventional CNTs (Figure 4e)).

We shall further discuss, in section D, the formation mechanism of HCNTs, and the subsequent transformation from HCNT(O)s to the hybrid CNT⊂HCNT nanostructures, and eventually to the conventional CNT(O)s.

(*2*) *The Templates: SiNWs and SiNDs*. We believe that hydrogen-terminated SiNWs and SiNDs serve as templates in the formation of carbon-based nanostructures. They facilitate the formation of the different types/shapes of carbon and hydrocarbon nanostructures. Indeed, control experiments without SiNWs, or with as-prepared SiNWs (which are covered with oxide), yielded little or no carbon nanomaterials. Furthermore, both HCNT(O)s and CNT(O)s have been observed with SiNW(D)s attached (hereafter designated as SiNW(D)⊂HCNT(O) and SiNW(D)⊂CNT(O), respectively). The demolded HCNT(O)s, CNT(O)s, or the hybrids often retain the shape of the template (with varying degree of shrinkage in the inner diameter as we shall discuss later).

(*3*) *Surface Speciation of SiNWs and SiNDs*. Etching of as-prepared SiNWs or SiNDs with HF gives rise to hydrogen-terminated SiNW(D) surfaces covered with SiH_x (where $x = 1-3$) species.[4] To investigate the crucial role played by these reactive surface moieties, we performed control experiments with as-prepared SiNW(D)s (covered with oxide). The results showed little or no carbon nanomaterials. Indeed, the reactions may be initiated and/or catalyzed by the surface Si−H moieties on the SiNW(D) surfaces. Under the extreme local temperatures within the acoustic cavity and in halogenated solvents such as $CHCl_3$ or CH_2Cl_2, the reaction between the Si−H and C−Cl moieties results in dehydrochlorination or dechlorination, giving rise to chemisorbed CH or CH_2 units that subsequently polymerize to form hydrogenated graphite sheets wrapping around SiNWs or SiNDs, thereby forming the HCNTs and HCNOs. Previous works by Nishihara et al.[18] also showed that electrochemical reduction of halogenated organic compounds could lead to carbonaceous or graphitic deposits.

(17) Suslick, K. S.; Price, G. J. *Annu. Rev. Mater. Sci.* **1999**, *29*, 295.
(18) Nishihara, H.; et al. *J. Chem. Soc., Faraday Trans.* **1991**, *87*, 1187.

Those electrodeposited materials typically had a molecular structure resembling turbostratic graphite.

(*4*) *Functionality of the Reactant: The "Solvent" Effect.* Most of the common organic solvents can be used as the source of the HCNT(O)s. However, the yield varies with the functionality of the solvent molecule. The solvents/reactants can be grouped into two broad categories. The first category (Class A) comprises organic solvents such as chloroform, methylene chloride, and benzene, etc., which are hydrophobic and immiscible with water. The second category (Class B) consists of solvents such as acetone, methanol, and ethanol, most of which are hydrophilic and miscible with water. Further subdivision can be done according to their functionality.

Our study indicates that the efficiency in producing the carbon nanomaterials depends critically on the dispersion of H-terminated SiNWs in the organic solvent and the reactivity of the solvent molecules on the hydrogen-terminated silicon surface (under sonication conditions).

With regards to the dispersion, HF-etched SiNWs disperse well in Class A solvents but not Class B solvents under sonication conditions. This observation is not unexpected and can be rationalized as follows. After HF-treatment, the SiNW surfaces are terminated by hydrogen atoms, forming surface SiH_x (x = 1,2,3) species.[4] Because SiH_x moieties are hydrophobic, it follows that the HF-etched SiNWs can be solvated and dispersed well in hydrophobic solvents. The degree of dispersion can be controlled by factors such as the concentration of the SiNW(D) solution, solvent type, sonication time and power, etc.

The reactivity depends on the functionality of the solvent. High reactivity can be found in select Class A solvents such as the halogenated hydrocarbons. Among them, chloroform, followed by methylene chloride, exhibits the highest reactivity and produces structurally well-defined hydrocarbon and carbon nanostructures, as depicted in Figures 2 and 3.

Interestingly, the relative propensity of halogen-substituted aliphatic hydrocarbons to give HCNT(O)s decreases with increasing carbon chain length, as indicated by our unpublished results on the following series, which exhibits the trend of iodomethane > 1,1,2,2-tetrabromoethane > 1-bromohexane. Here the long-chain *n*-hexyl bromide produced very little carbon nanomaterials. We therefore conclude that the best halogen-substituted aliphatic hydrocarbons are those with one carbon unit and several halogen atoms, i.e., the series of CH_3X, CH_2X_2, and CHX_3. Within this group, the relative propensity seems to follow the general trends of $CH_3X < CH_2X_2 < CHX_3$ and Cl < Br < I. These observations are consistent with our proposed mechanism (to be described in the next subsection) which requires the departure of the halogen atom(s) as the leaving group (note that I is a better leaving group than Br and Cl) and the formation of basic CH units on the silicon surface as the first step (vide infra).

However, not all Class A solvents are good candidates. For example, unsubstituted aliphatic hydrocarbons such as hexane are not good sources. The same is true for certain halogenated solvents. The most interesting example is CCl_4, which is a Class A and halogen-containing solvent. Yet it exhibits low reactivity with very little carbon nanomaterials formed, even under prolonged sonication. This observation is also in line with our proposed mechanism (vide infra). Specifically, the lack of hydrogen atoms in CCl_4 may have precluded the formation of C−H units on the surfaces of SiNWs, which is believed to be the key initial step in the formation of these nanomaterials.

Surprisingly, aromatic hydrocarbons such as benzene (also a Class A solvent) are not as good as chloroform or methylene chloride in producing HCNT(O)s upon sonication in the presence of SiNW(D)s. To probe the formation mechanism of HCNTs in different solvents, and the subsequent transformation from HCNTs to CNTs via the hybrid nanostructures, we also studied the HRTEM images of HF-etched SiNWs in benzene as a function of sonication time, namely, from 10 to 20 to 30 min. (but otherwise under the same conditions). The reactions are much slower than in chloroform and the products, including HCNTs or the hybrid CNT⊂HCNT nanostructures, are often irregular in shape. Typical HRTEM images are portrayed in Figure 5a−c, respectively. It can be seen that only an amorphous carbon layer was obtained after 10 min sonication. Further sonication caused the germination of HCNT layers on top of amorphous hydrocarbon layer of wavy HCNT layers, as depicted in Figure 5b. After prolonged sonication (30 min), irregular-shape hybrid CNT⊂HCNT nanostructures were formed (see Figure 5c).

These observation can be rationalized as follows. Though benzene contains C−H units, chemisorption of benzene rings on the surfaces of SiNWs gives rise to stereochemical constraints that hinder the formation of the HCNT layers. Hence the reactions are much slower than that in chloroform and the products are frequently irregular in shape. Such constraints are absent in the case of free chemisorption C−H units as for $CHCl_3$.

We have also investigated a number of Class A solvents with different structures and functionalities. One example is cyclic oxygen-containing solvents such as THF, 1,4-dioxane. These latter solvents produced irregular-shaped HCNT(O)s in low yields. A more detailed report of the "solvent" effect will be forthcoming.

D. Formation of HCNT(O)s and Their Transformation into CNT(O)s via Hybrid CNT(O)⊂HCNT(O) Intermediates. On the basis of detailed TEM observations and the spectroscopic evidence, we propose the following mechanism for the formation of HCNT(O)s and their transformation into CNT(O)s on hydrogen-passivated SiNW(D)s via the hybrid nanostructures as intermediates. We should emphasize that the new experimental observation of the intermediate hybrid nanostructures provides a more detailed picture of the mechanism than that previously proposed by us.[1,2]

(*1*) *Mechanism for the Formation of HCNT(O)s.* Previously, it was proposed by us[1,2] that carbon nanotube/nano-onion nucleation occurs at the active sites on the

surfaces of silicon nanowires/nanodots, respectively. The active sites contain SiH_x species which, under the ultrasonication conditions, promote the formation of the basic structural units of carbon derived from the organic solvent. While these heterogeneous reactions may be rather complicated, they may be represented as

$$(HC)_{ad} \xrightarrow[SiNW(D)]{\text{sonication}} \text{a-}(HC)_x \xrightarrow[SiNW(D)]{\text{sonication}} HCNT + HCNO \quad (1)$$

Here $(HC)_{ad}$ denotes the adsorbed hydrocarbon units on the surfaces of SiNWs or silicon nanodots (SiNDs) (hereafter referred to collectively as SiNW(D)s) and a-$(HC)_x$ represents the polymerized amorphous hydrocarbon fragments. These hydrocarbon polymer fragments may be likened to hydrogenated amorphous carbon (a-C:H) on one hand and hydrogenated graphite on the other. The joining of hydrogenated graphitic fragments eventually forms wavy layers of HCNT(O)s. In other words, polymerization of these basic units results in the formation of graphene sheets which wrap around SiNW(D) (the mold). The transformation from chemisorbed amorphous hydrocarbon a-$(HC)_x$ to HCNT(O)s can be seen from Figure 4a to Figure 4b for $CHCl_3$. Even more striking is the genesis of the formation of HCNT layers on top of the chemisorbed amorphous hydrocarbon layers in going from Figure 5a to Figure 5b for benzene.

Support of the above mechanism also comes from works by others. For example, experimentally it was observed that amorphous carbon nanowires (a-CNW) can be converted to MWCNTs upon annealing at 900 °C.[19] As pointed out by the authors: (1) these a-CNWs also contain C−H bonds; and (2) despite its amorphous nature as revealed by HRTEM, these a-CNWs actually contain graphitic building blocks that can polymerize to form highly distorted MWCNTs upon annealing at high temperatures. Our proposed mechanism is also consistent with the following observations reported in the literature: (1) MWCNOs can be formed by heating amorphous carbon film with an electron beam[9] and (2) graphitic carbon film can be formed by heating an amorphous carbon film.[20]

The role of Si−H bonds on the surfaces of silicon nanowires/nanodots in the sonochemical synthesis of HCNT(O)s deserves further comments. In fact, fabrication of organic materials on clean or hydrogen-passivated silicon surfaces is not new. In recent years, a variety of the functionalization approaches for formation of structurally and chemically well-defined organic monolayers on clean or hydrogenated silicon (or porous silicon) surfaces in vacuum or in solution have been developed.[21,22] For example, radical-initiated hydrosilylation, thermal-driven hydrosilylation, photolytic hydrosilylation, etc., of unsaturated carbon compounds have been reported. Most related to our case is the thermal-induced hydrosilylation of alkenes and alkynes.

In the absence of radical initiator, hydrosilylation through homolytic cleavage of Si−H bonds can occur at a temperature higher than that for radical-initiated hydrosilylation. The high temperature, generally 150−200 °C, promotes homolytic cleavage of Si−H to generate silicon radicals or dangling bonds (Si−H → Si•+ •H) on silicon surfaces.[23,24] Such a Si• radical can react with an unsaturated bond (as in an alkene) to form an alkyl group on the silicon surface via Si−C bond formation and abstraction of a hydrogen atom from an adjacent silicon site. These radical chain reactions can thus propagate on the silicon surface, just as that of radical-initiated reactions.[25,26] Aliphatic monolayers thus produced on hydrogen-terminated Si surfaces are stable up to 350 °C in a vacuum.[27]

Thermally induced hydrosilylation of alkenes (as well as alkynes) has also been applied to hydrogen-terminated porous silicon surfaces, producing passivating aliphatic monolayers via the same mechanism as in the case of flat (crystalline) silicon surfaces.[28,29] These latter studies are particularly relevant to the present study in that porous silicons are known to contain silicon nanowires and nanodots. In view of the extremely high local temperature within the acoustic cavitation of ultrasound (vide supra), we believe that a similar radical mechanism (i.e., homolytic cleavage of Si−H conds) occur at the nucleation site(s) on the silicon surfaces of silicon nanowires and nanodots. Such a Si• radical can react with a chemisorbed organic molecule such as chloroform to form the basic carbon units which then polymerize to form a hydrogenated graphene sheet wrapping around the SiNW(D)s. In the latter process, the interfacial Si−C bonds are eventually severed and replaced by the much stronger C−C bonds of the hydrogenated graphene sheet. Finally, propagation of these free radical chain reactions gives rise to the multilayer HCNT(O)s.

Chemical binding of benzene on Si(100) surface at 300 K, via Si−C σ bond formation, has also been thoroughly investigated.[30,31] Two chemisorption states with desorption peaks at 432−460 and 500 K were found.

(19) Tang, Y. H.; Zhang, P.; Kim, P. S.; Sham, T. K.; Hu, Y. F.; Sun, X. H.; Wong, N. B.; Fung, M. K.; Zheng, Y. F.; Lee, C. S.; Lee, S. T. *Appl. Phys. Lett.* **2001**, *79*, 3773.
(20) Wesner, D.; Krummacher, S.; Carr, R.; Sham, T. K.; Strongin, M.; Eberhart, W.; Weng, S. L.; Willaims, G.; Howells, M.; Kampas, F.; Head, S.; Smith, F. W. *Phys. Rev. B* **1983**, *28*, 2152.
(21) Tao, F.; Bernasek, S. L.; Xu, G.-Q. Chem. Rev. **2009**, *109*, 3991, and references cited therein.
(22) Buriak, J. M. Chem. Rev. **2002**, *102*, 1271, and references cited therein.
(23) Sano, H.; Maeda, H.; Matsuoka, S.; Lee, K. H.; Murase, K.; Sugimura, H. *Jpn. J. Appl. Phys.* **2008**, *47*, 5659.
(24) Labinger, J. A. In *Comprehensive Organic Synthesis*; Trost, B. M., Fleming, I., Eds.; Pergamon: New York, 1991;Vol. *8*, p 699.
(25) Linford, M. R.; Chidsey, C. E. D. *J. Am. Chem. Soc.* **1993**, *115*, 12631.
(26) Linford, M. R.; Fenter, P.; Eisenberger, P. M.; Chidsey, C. E. D. *J. Am. Chem. Soc.* **1995**, *117*, 3145.
(27) Sung, M. M.; Kluth, J.; Yauw, O. W.; Maboudian, R. *Langmuir* **1997**, *13*, 6164.
(28) Bateman, J. E.; Eagling, R. D.; Worrall, D. R.; Horrocks, B. R.; Houlton, A. *Angew. Chem., Int. Ed.* **1998**, *37*, 2683.
(29) Boukherroub, R.; Morin, S.; Wayner, D. D. M.; Bensebaa, F.; Sproule, G. I.; Baribeau, J.-M.; Lockwood, D. J. *Chem. Mater.* **2001**, *13*, 2002.
(30) Taguchi, Y.; Fujisawa, M.; Takaoka, T.; Okada, T.; Nishijima, M. *J. Chem. Phys.* **1991**, *95*, 6870.
(31) Fink, A.; Menzel, D.; Widdra, W. *J. Phys.Chem. B* **2001**, *105*, 3828.

These studies point to the disruption of the strong π system of aromatic molecules such as benzene and the formation of Si−C sigma bonds upon chemisorption on the silicon surface. Under sonication conditions, the thermally generated Si• radicals on the silicon surface can initiate Si−C σ bond formation and transfer the unpaired electron to the π system. The free radical can then propagate through the aromatic π system, giving rise to C−C sigma formation between benzene molecules, thereby producing the hydrogenated graphene sheet through radical chain reactions, and eventually giving rise to the multilayer HCNT(O)s, in a way similar to that described earlier for chloroform.

The major differences between of our system (referred to as System A) and the aliphatic monolayers produced via hydrosilylation on hydrogen-terminated Si surfaces (referred to as System B) mentioned earlier are: (1) the reactants: System A uses small hydrophobic organic molecules (such as chloroform) whereas System B requires unsaturated compounds (such as alkenes); (2) the reaction conditions: System A uses room-temperature and atmospheric reaction conditions whereas System B requires high temperature of 150−200 °C; (3) the products: System A allows fabrication of multilayer hydrocarbon nanotubes or nano-onions HCNT(O)s, whereas System B produces organic monolayers; (4) stability of the products: HCNT(O)s are unstable under sonication conditions; they can transform into conventional CNT(O)s and/or extrude (demold) from the SiNW(D)s upon sonication (as we shall describe in the next section). They are, however, stable indefinitely under ambient conditions. Aliphatic monolayers produced on hydrogen-terminated Si surfaces through thermal hydrosilylation of alkenes are stable up to 350 °C (as discussed above), thereby serving as a passivation layer.

(*2*) *Transformation from HCNT(O)s to CNT(O)s via Hybrid HCNT(O)/CNT(O) Intermediates*. It was during the preparation of HCNTs and HCNOs that we discovered the hybrid HCNT/CNT nanostructures depicted in Figure 1−3. A general characteristic of these hybrid nanostructures is that they consist of a few inner CNT layers, with uniform interlayer spacing of 3.4 Å and a number of outer, wavy HCNT layers with variable interlayer spacing of 4−6 Å. Because prolonged sonication can convert HCNT(O)s into conventional CNT(O)s, we conclude that these hybrid nanostructures are the intermediates in the following transformation process under sonication

$$\mathrm{HCNT(O)} \xrightarrow{\text{sonication}} \text{(hybrid)CNT(O)} \subset \mathrm{HCNT(O)} \xrightarrow{\text{sonication}} \mathrm{CNT(O)} \quad (2)$$

As expected, the relative proportions of HCNT(O)s, the hybrid intermediates, and the end products CNT(O)s change with sonication time and acoustic power. Figure 4b−e shows the HRTEM images of selected products from $CHCl_3$ as a function of the sonication time, ranging from zero (stirring only) to 20 min. The transformation from HCNT(O)s to hybrid intermediates to CNT(O)s is readily apparent. The same is true for benzene, as is evident in going from Figure 5a to Figure 5c. We should note that sonication promotes reactions 1 and 2 and causes the transformation from chemisorbed amorphous hydrocarbon $(HC)_{ad}$ units to polymerized amorphous hydrocarbon fragments a-$(HC)_x$ to HCNT(O)s to hybrid intermediates to CNT(O)s. As the sonication time increases, the relative yields of these products change according to these reactions.

(*3*) *Inside-out or Outside-in Conversion?* The question naturally arises as to whether the HCNT(O) to CNT(O) conversion process begins with the innermost layers (on the SiNW(D) surface) and propagates outward (the "inside-out" mode) or the opposite (the "outside-in" mode). Detailed observation under HRTEM as a function of time revealed that the inner wavy HCNT layers get converted to CNT layers first, and such transformation propagates outward to the outer layers upon prolonged sonication. Typical examples are shown in Figure 1. Hence they may be described as CNT(O)s encapsulated within HCNT(O)s, i.e., (hybrid)CNT(O)⊂HCNT(O) or simply CNT(O)⊂HCNT(O). Subsequent annealing under sonication conditions produces smoother CNT layers. This conversion can happen with or without the SiNW(D)s attached (i.e., before and after demolding).

(*4*) *The Extrusion* (*Demolding*) *Processes*. Further sonication causes SiNW(D)s to shed off HCNT(O)s, refreshing SiNW surfaces for further reactions. Experimentally, it was observed that the demolding process can occur at any stage of the formation or transformation of the carbon nanomaterials (i.e., at the HCNT, CNT, or hybrid stages), as illustrated in eqs 3−5.

$$\mathrm{SiNW(D)} \subset \mathrm{HCNT(O)} \xrightarrow{\text{sonication}} \mathrm{SiNW(D)} + \mathrm{HCNT(O)} \quad (3)$$

$$\mathrm{SiNW(D)} \subset \mathrm{CNT(O)} \subset \mathrm{HCNT(O)} \xrightarrow{\text{sonication}} \mathrm{SiNW(D)} + \mathrm{CNT(O)} \subset \mathrm{HCNT(O)} \quad (4)$$

$$\mathrm{SiNW(D)} \subset \mathrm{CNT(O)} \xrightarrow{\text{sonication}} \mathrm{SiNW(D)} + \mathrm{CNT(O)} \quad (5)$$

E. Structure Model and Spectroscopic Evidence. We believe that the new structures of HCNTs/HCNOs are formed by networks of chair-form cyclohexane-like hexagonal structure, similar to that of partially hydrogenated graphite on the one extreme and that of amorphous hydrocarbon (a-C:H) on the other. Morphologically, they are similar to the conventional CNTs or CNOs except that C−H bonds have been inserted between layers (walls), thereby converting curved sp^2 layers into puckered sp^3 layers. Obviously, the more C−H bonds are inserted, the larger will be the interlayer spacing. The interlayer spacing also depends on the degree of packing between adjacent layers. As we saw in the HRTEM

images (cf. Figures 1−5), the interlayer spacing can vary from 3.4 to 6 Å.

This structure model is supported by a number of spectroscopic evidence. Raman and electron energy loss spectra (EELS) had been discussed in ref 2. We shall give a more detailed discussion of the Raman spectrum in the 1100−1800 cm^{-1} region and a new Raman spectrum in the 100−1100 cm^{-1} region (Figure 6), followed by a new ATR-FTIR spectrum (Figure 7). Figures 6 and 7 are reported here for the first time.

In the range of 1100−1800 cm^{-1}, there are three weak Raman scattering peaks (excitation: 514 nm) at 1300, 1450, and 1600 cm^{-1}, shown in Figure 8 of ref 2. The peak at 1300 cm^{-1} can be assigned to sp^3−hybridized single C−C bond, whereas that at 1600 cm^{-1} is consistent with sp^2−hybridized double C═C bond, stretching frequencies of HCNT(O)s. These bands are very different from those of conventional CNTs which generally have a strong so-called graphitic G-band at 1580 cm^{-1} (sp^2 hybridized, C═C stretch) and a much weaker, so-called disorder-induced, D-band at 1348 cm^{-1} (sp^3 hybridized, C−C stretch). The ratio of the intensities of these bands, D/G, for our samples is about one (1), in sharp contrast to that of ca. 0.15 in most CNTs,[32−35] consistent with the notion that most of the carbon atoms are hydrogenated (i.e., sp^3 hybridized carbons with C−H bonds). Note that the characteristic Raman peak of diamond is at 1332 cm^{-1}, which should serve as the benchmark for sp^3 hybridized C−C bonds. The peak at 1450 cm^{-1} is most interesting. It has not been observed in any CNTs, single- or multiwalled. We have assigned it to a C−C stretch with a formal bond order of 1.5. However, we cannot rule out the possibility of this peak being due to a C−H bending mode. Indeed, the shoulders at 1330, 1350, and 1370 cm^{-1} (weak peaks) are most likely due to certain vibration modes of C−H bonds.

In the Raman region of 100−1100 cm^{-1}, there are two intense peaks at 517 cm^{-1} and 960 cm,$^{-1}$ as depicted in Figure 6. These peaks can be attributed to the scattering of the first-order optical phonon and the overtone of TO (L) of Si in SiNW(D)s, respectively.[36] The peak at 300 cm^{-1} is also due to silicon. Like multiwalled CNTs,[32−35] no discernible peaks were observed for multiwalled HCNTs in the region of 150−380 cm^{-1} expected for the radial breathing modes (RBM).

The ATR-FTIR spectrum of a typical HCNT/CNT sample is shown in Figure 7. The C−H stretching frequencies at ca. 2960, 2925, and 2855 cm^{-1} can clearly be seen. The C−C and C═C bands at 1263 and 1648 cm^{-1}, respectively, as well as the intermediate peak at 1458 cm^{-1}, are in agreement with these observed in the Raman spectrum described above. The differences in wave numbers of IR vs Raman spectra can be attributed to the different ratios of HCNT vs CNT in the samples. Also observed in the IR spectrum is the peak at 1725 cm^{-1} which may be assigned to C═C (or C═O) stretching frequencies. Interestingly, there are two broad (unresolved) Si−H bands in the FTIR at ca. 2100 and 2250 cm^{-1}, the former being due to unoxidized H-terminated silicon surface, whereas the latter is attributable to oxidized H-terminated silicon surface (i.e., O_3Si-H). The fact that both unoxidized and oxidized H-terminated silicon surfaces are present is also evident in the region around 1000 cm^{-1}. Here three absorption peaks are observed: 910 cm^{-1} due to unoxidized H-terminated silicon surfaces ($Si-H_x$ scissoring modes), and 1050 (in-plane Si−O−Si stretching mode) and 800 (in-plane Si−O−Si bending mode) due to oxidized silicon surfaces.[4,37]

F. Other Interesting Properties and/or Phenomena. Several other interesting phenomena and/or observations are worth mentioning here.

(*1*) *Shrinkage Upon Demolding*. Upon demolding, the inner and outer diameters of the extruded HCNT(O) or CNT(O) usually shrink by a factor of 2 or more. Some even collapse completely to form a more-or-less solid multiwalled tube or onion. Deformation of the morphologies can also occur in the demolding process, depending upon the types and shapes of the silicon template (mold).

It should be emphasized that, upon demolding, the inner diameters (3−5 nm) of the partially collapsed HCNT(O)s or CNT(O)s are, in general, much smaller than the diameters (10−20 nm) of the SiNW(D) molds because of the shrinkage. And, as expected, for the same SiNW(D) mold, the shrinkage is substantially less for the structurally more rigid CNT(O)s than the HCNT(O)s. Examples can be found in ref 2.

(*2*) *Explosive Outgassing*. Distinct breaks or pinholes can sometimes be observed on the walls or shells of CNT(O)s or HCNT(O)s. These breaks are believed to be due to "explosive" outgasing caused by either the sonication process or electron irradiation during TEM observation, or both. These "explosions" can be likened to "volcanic eruptions" of gaseous materials from the earth crest. The gaseous materials could either be hydrogen molecules released as a result of the dehydrogenation process during the HCNT(O)-to-CNT(O) transformation or some foreign materials trapped within the shells or inside HCNT(O) or CNT(O). As indicated by the white arrows in Figure 8, there are a few tracks radiating from the center of the nano-onion to the outermost shell. Many similar breaks can also be seen in the HCNT(O)/CNT(O)s depicted in Figures 1 and 3. Some exit points of these tracks on the outermost shell even show severe bulging and/or damage caused by the explosions.

(*3*) *Self-Sealing and Self-Healing of Nanotubes and Nano-onions*. As described earlier,[2] HCNT(O)s are more

(32) Dresselhaus, M. S.; Dresselhaus, G; Saito, R.; Jorio, A. *Phys. Rep.* **2005**, *47*, 409.
(33) Jorio, A.; Saito, R.; Hafner, J. H.; Lieber, C. M.; Hunter, M.; McClure, T.; Dresselhaus, G.; Dresselhaus, M. S. *Phys. Rev. Lett.* **2001**, *86*, 1118.
(34) Christofilos, D.; Arvanitidis1, J.; Efthimiopoulos, E.; Zhao, X.; Ando, Y.; Takenobu, T.; Iwasa, Y.; Kataura, H.; Ves, S.; Kourouklis, G. A. *Phys. Status Solidi B* **2007**, *244*, 4082.
(35) Costa, S.; Borowiak-Palen, E.; Kruszynska, M.; Bachmatiuk, A.; Kalenczuk, R. J. *Mater. Sci.* (*Poland*) **2008**, *26*, 433.
(36) Zhang, Y. F.; Tang, Y. H.; Wang, N.; Yu, D. P.; Lee, C. S.; Bello, I.; Lee, S. T. *Appl. Phys. Lett.* **1998**, *72*, 1835.
(37) Tsybeskov, L; Fauchet, P. M. *Appl. Phys. Lett.* **1994**, *64*, 1983.

fragile than CNT(O)s and can easily damage, shrink, or break under intense electron beam during TEM examination. In fact, when a HCNT breaks, the broken ends often "self heal" to form two half "bucky" caps, thereby sealing the broken ends of the separated tubes. This phenomenon is illustrated in Figure 9. Depending upon the intensity of the electron beam, the "caps" could be in the form of one, two, or more bucky spheres of decreasing diameters fused together at the end of the tubes, resulting in morphologies resembling the shapes of stalactites or icicles. One example is depicted in Figure 9b, which originated from the tube portrayed in Figure 9a after being broken into two HCNTs by electron beam irradiation. A separate, badly damaged, sealed-off tube hanging out of a SiNW is shown in Figure 9c.

(*4*) *Deformation*. Without the internal support of the encapsulated SiNW(D)s (the molds), the HCNT(O)s, and to a lesser extent, the CNT(O)s, tend to deform to form polyhedral shapes upon demolding, as exemplified by the various nanostructures portrayed in Figures 2 and 3. This "polyhedralization" phenomenon is also intimately related to the formation of faceted tubes or polyhedral onions discussed above (see also discussions in section G).

G. Other Transformations and Interconversions. (*1*) *Transformations from Round to Faceted Nanostructures*. We also found that prolonged ultrasonication can convert demolded HCNT(O)s or CNT(O)s into faceted HCNT(O)s and faceted CNT(O)s ((hereafter designated as f-HCNT(O)s) and f-CNT(O)s), respectively). Examples are portrayed in Figures 2 and 3. Obviously this process can only happen after demolding. These observations are similar to the well-known conversion of "bucky onion" into faceted or polyhedral bucky onions.[8]

$$\text{HCNT(O)} \xrightarrow{\text{sonication}} \text{faceted-HCNT(O)} \qquad (6)$$

$$\text{CNT(O)} \xrightarrow{\text{sonication}} \text{faceted-CNT(O)} \qquad (7)$$

(*2*) *Transformations from Nanotubes to nano-onions*. We also found that electron beam irradiation of HCNTs (after demolding) can cause buckling or collapse of the tubular structure and, under favorable conditions, result in the formation of HCNOs

$$\text{HCNT} \xrightarrow{\text{electronirradiation}} \text{HCNO} \qquad (8)$$

Similar transformation from CNTs to CNOs (eq 9) upon intense electron beam irradiation can also be formed in the literature[9]

$$\text{CNT} \xrightarrow{\text{electronirradiation}} \text{CNO} \qquad (9)$$

It was first discovered by Ugarte that when carbon nanotubes are irradiated with intense electron beam, the tubular structures of the MWCNTs can collapse to form spherical, onionlike carbon nanoparticles (called buckyonions), which consist of nested concentric spherical graphitic layers. Further electron beam irradiation can lead to faceted structures as discussed in the previous subsection.

Conclusions

This paper reports an intermediate form of carbon nanomaterials which may be described as the hybrid of conventional carbon nanotubes (CNTs) and hydrocarbon nanotubes (HCNTs), as well as the hybrid of conventional nano-onions (CNOs) and hydrocarbon nano-onions (HCNOs). More importantly, it was found that HCNTs and HCNOs can be converted to CNTs and CNOs upon prolonged sonication, under ambient conditions, with the hybrid CNT/HCNT and CNO/HCNO nanostructures as intermediates, respectively. These intermediate hybrid carbon nanostructures may thus be considered as snapshots in the transformation process. The morphologies and the characteristic properties of these carbon nanostructures are reported. Four key components in the sonochemical synthesis of HCNT(O)s, CNT(O)s, and the hybrid intermediates were identified. The characteristics of HCNT(O)s, which distinguish them from the conventional CNT(O)s, are described. The formation of HCNT(O)s, and the subsequent transformation from HCNT(O)s to the hybrid CNT(O)⊂HCNT(O) nanostructures, and ultimately to the conventional CNT(O)s, have been elucidated by recording the HRTEM images of the products as a function of sonication time and in different solvents. On the basis of these experimental results, detailed formation mechanism and transformation pathways of these carbon nanomaterials, as well as their interrelationships, are proposed. A detailed comparison of the mechanism proposed here for the formation of HCNT(O)s on SiNW(D)s and that for the fabrication of passivating organic monolayers on 2D silicon surfaces (or porous silicon) via hydrosilylation is made. Structural models of HCNT(O)s are proposed. Other peculiar phenomena and transformation processes of these carbon nanomaterials as well as the molding and demolding processes under sonolysis conditions are also described.

Acknowledgment. This work was supported by the Collaborative Research Grants, Research Grants Council of Hong Kong (CityU5/CRF/08). N.B.W. acknowledges the support of a Strategic Grant (Project 7002353) from the City University of Hong Kong.